Group	BV/TV (%)	P		Tb.Th (mm)	P		Tb.Sp (mm)	P		Tb.N (1/mm)	P	
Sham	0.30±0.07			0.064±0.005			0.161±0.035			6.82±1.60		
OVX vehicle	0.14±0.07		†††	0.053±0.010		†	0.344±0.079		†††	3.33±1.27		†††
OVX risedronate 0.1 mg/kg per day	0.16±0.06	NS	††	0.061±0.009	*	NS	0.292±0.087	NS	††	3.96±1.56	NS	†
OVX risedronate 0.5 mg/kg per day	0.20±0.06	*	†	0.064±0.007	**	NS	0.184±0.045	***	NS	5.88±1.72	**	NS
OVX risedronate 2.5 mg/kg per day	0.59±0.21	***	††	0.076±0.009	***	††	0.074±0.043	***	†††	13.85±3.99	***	†††
Group	SMI	P		DA	P		Conn.D (1/mm^3)	P				
Sham	0.72±0.48			1.84±0.12			180.0±76.9					
OVX vehicle	1.79±0.41		†††	1.98±0.19		NS	34.3±44.2		†††			
OVX risedronate 0.1 mg/kg per day	1.92±0.49	NS	†††	1.86±0.18	NS	NS	63.6±57.1	NS	††			
OVX risedronate 0.5 mg/kg per day	−2.22±0.49	***	†††	1.75±0.08	**	NS	148.0±111.7	**	NS			
OVX risedronate 2.5 mg/kg per day	−3.93±4.86	**	†	1.63±0.05	***	††	782.7±55.2	***	†††			

*P<0.05, **P<0.01, ***P<0.001: significantly different for OVX vehicle group

†P<0.05, ††P<0.01, †††P<0.001: significantly different for sham group

Effect of risedronate on trabecular biomechanical properties

The effect of risedronate on biomechanical properties of trabecular bone was investigated by FEA, since compression testing of trabecular bone of the tibia is difficult. The microstructural parameters in the cubic bone region extracted for FEA (VOI-2) (Fig. 2) correlated highly with those in the whole trabecular bone region (VOI-1) (P<0.0001 for BV/TV, connectivity density, SMI, Tb.N, Tb.Th, and Tb.Sp and P<0.05 for DA). The magnitude of changes in this cubic region was greater than in the whole trabecular region for OVX as well as treatment groups (data not shown).

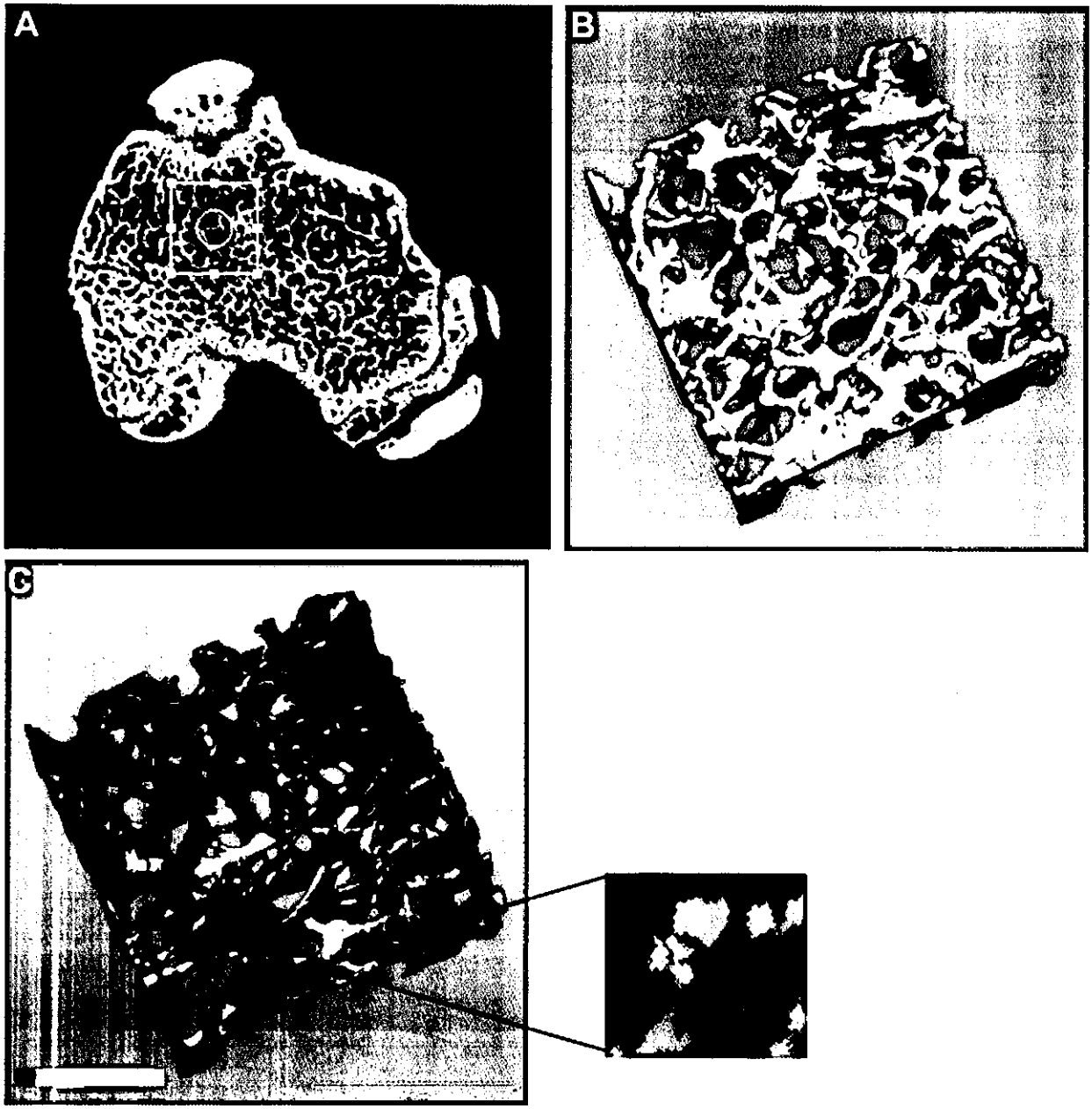

Fig. 2A–C Compression and shear simulation of three orthogonal directions. **A** The region of proximal tibia that was extracted for finite element analysis is shown. *The circle in the center* of the cubic region indicates the region that we used for calculating the degree of anisotropy. **B** The original 3D micro-CT image (upper half of the total region). **C** The 3D distribution image of von Mises stress (upper half of the total region). A high-stress region is highlighted in red in the magnified view.

Table 2 shows Young's and shear moduli in the maximal principal direction in OVX rats and risedronate-treated OVX rats. OVX caused a significant decrease in Young's modulus, and tended to decrease shear modulus, compared with the sham group. Treatment with risedronate at the dose of 2.5 mg/kg significantly increased Young's and shear moduli, even above the values of the sham group. When mechanical DA was calculated as the ratio of the largest Young's modulus divided by the third Young's modulus, it was increased by OVX and was decreased by treatment with risedronate (Table 2).

Table 2 Biomechanical parameters in the sham and OVX rats treated with risedronate (mechanical DA = the largest Young's modulus/the third Young's modulus, *NS* not significant)

Group	Young's modulus	P		Shear modulus	P		Mechanical DA	P	
Sham	1,074±454			208±154			6.4±5.6		
OVX vehicle	361±300		††	82±105		NS	82.8±58.5		†
OVX risedronate 0.1 mg/kg per day	527±257	NS	††	72±67	NS	†	74.1±65.0	NS	††
OVX risedronate 0.5 mg/kg per day	638±161	NS	†	93±125	NS	NS	20.0±24.8	**	NS
OVX risedronate 2.5 mg/kg per day	3,691±1,555	** *	†† †	1,163±682	** *	†† †	2.7±3.3	***	NS

*P<0.05, **P<0.01, ***P<0.001: significantly different for OVX vehicle

†P<0.05, ††P<0.01, †††P<0.001: significantly different for sham group

Correlation between microstructural changes and biomechanical properties

Table 3 summarizes the results of multiple linear regression analysis to see how BV/TV and microstructural parameters contribute to bone strength. BV/TV correlated highly with Young's modulus in sham and risedronate groups at 0.5 mg/kg and 2.5 mg/kg (R^2=0.73–0.84). In the sham group, the addition of structural parameters did not affect Young's modulus. In contrast, in risedronate at 0.5 mg/kg and 2.5 mg/kg the correlation was increased substantially by the addition of structural parameters to BV/TV, notably SMI and connectivity density (R^2=0.88 in risedronate (RIS) 0.5 mg/kg, R^2=0.93 in RIS 2.5 mg/kg).

Table 3 R^2 values of multiple linear regression analysis between microstructural parameters and biomechanical properties in individual groups. *R^2(BV/TV)* the coefficient of biomechanical properties with BV/TV, *R^2(BV/TV +)* the coefficient of biomechanical properties with BV/TV and another microstructural parameter. Values are shown when their *P* values were significant (P<0.05)

Parameter	Sham		OVX		RIS 0.1			RIS 0.5			RIS 2.5		
	R^2 (BV/TV)	R^2 (BV/TV +)	R^2 (BV/TV)	R^2 (BV/TV +)	R^2 (BV/TV)	R^2(BV/TV +)		R^2 (BV/TV)	R^2(BV/TV +)		R^2 (BV/TV)	R^2(BV/TV +)	
Young's modulus	0.85		0.56*		0.63	SMI	0.75	0.73	SMI	0.88	0.80	SMI	0.93
						ConnD	0.74		ConnD	0.88		ConnD	0.93
									Tb.N	0.84		Tb.Th	0.90
												Tb.Sp	0.90
												Tb.N	0.88
	R^2 (BV/TV)	R^2 (BV/TV +)	R^2 (BV/TV)		R^2 (BV/TV)	R^2(BV/TV +)		R^2 (BV/TV)	R^2(BV/TV +)		R^2 (BV/TV)	R^2(BV/TV +)	
Shear modulus	0.85		0.48*		0.69	SMI	0.82	0.74	ConnD	0.90	0.84	SMI	0.99
						ConnD	0.81		SMI	0.89		ConnD	0.98
						Tb.Sp	0.77		Tb.N	0.82		Tb.Sp	0.92
						Tb.N	0.75						

*The P values of R^2 were not significant (P>0.05)

Discussion

Microstructural deterioration caused by estrogen deficiency is characterized by progression of localized trabecular surface resorption [7], and SMI and connectivity density are considered to be the most sensitive parameters to reveal surface contour and disconnectivity of trabeculae, respectively. In the current study we found the impact of risedronate treatment on the trabecular microstructure of OVX rat. Multiple linear regression analysis revealed a strong correlation of SMI and connectivity density with Young's modulus as well as the shear modulus. The combination of BV/TV with SMI or connectivity density explained 90% of changes in Young's modulus or shear modulus. A previous study on the effect of risedronate in calcium-deficient OVX minipigs [3] showed that BV/TV alone could explain 76% of the observed variability in bone strength and that the combination of bone volume and architectural variables accounted for >90% of mechanical strength. Although the animals used (minipig vs rat) and skeletal sites examined (vertebra vs tibia) differ, our results are consistent with those of their study.

In the sham group BV/TV alone showed high correlation with Young's modulus and shear modulus, and the addition of trabecular microstructural parameters did not increase correlation, suggesting that it is mainly bone volume that determines mechanical property under physiological conditions. In contrast, in OVX rats, neither BV/TV nor trabecular microstructural parameters showed high correlation with biomechanical properties. We observed in our previous experiments that OVX induced marked structural deterioration in the central part of spongiosa while relatively preserving the structure at the peripheral part of spongiosa close to the cortex of the tibia [18]. FEA in the present study was performed at the central part of the tibial metaphysis, where isolated, segmented structures existed in the OVX group. Thus, there may be dissociation between microstructural parameters calculated at the central region with deteriorated trabecular structure and parameters that are involved in bone strength.

In risedronate-treated group, the addition of microstructural parameters to BV/TV significantly increased correlation with bone strength, suggesting that alterations in 3D structure contribute to improvements in the biomechanical property by the drug. Risedronate may have the potential to remodel trabecular structure so that it can adapt to greater mechanical stress. Treatment with risedronate decreased the mechanical DA, which was increased by OVX, suggesting that risedronate maintained the biomechanical balance in any direction.

Our results suggest that an important mechanism underlying the biomechanical efficacy of risedronate in trabecular bone is to maintain the shape of trabeculae and their connectivity. This concept is supported by a previous histomorphometric study [19] on female beagles treated with risedronate (0.1, 0.5, or 2.5 mg/kg per day orally) showing that risedronate decreased final erosion depth at doses of 0.5 and 2.5 mg/kg and reduced activation frequency at 2.5 mg/kg. Bisphosphonates bind preferentially to sites of active resorption (where bone mineral or hydroxyapatite is exposed) [20] and inhibit osteoclast-mediated bone resorption. Bisphosphonates act to prevent bone loss at resorption sites, thereby preventing localized thinning of trabeculae and deterioration of 3D microstructure.

A limitation of this study was that the effect of mineralization on bone strength was not taken into account. The micro-CT based FEA determines mechanical property on the basis of the structure, not on the change in mineralization, which is affected by treatment with bisphosphonate [21]. In the future, higher resolution 3D images such as synchrotron radiation CT will provide more accurate information on mechanical property from the aspects of both structure and mineralization.

In conclusion, our results support the concept that, in addition to increasing bone mass, risedronate improve bone biomechanical properties through alterations of trabecular structure, especially its shape and connectivity. Coupled microstructural and micro-finite element analyses provide a useful tool for us to understand the mechanism of action of anti-resorptive agents, such as risedronate, from the perspective of how micro-architecture impacts on biomechanical property.

Acknowledgements We thank Dr. Kyoji Ikeda (Department of Bone and Joint Disease, The Research Institute, National Center for Geriatrics and Gerontology) for suggestions on the manuscript. We are grateful for the assistance of Mr. Jun Kono (Department of Radiology, Nagasaki Saiseikai Hospital). This study was supported in part by the Program for Promotion of Fundamental Studies in Health Science of the Organization for Pharmaceutical Safety and Research of Japan [Masako Ito (no. MF-14)] and by grant-in-aid for scientific research from the Ministry of Education in Japan [Masako Ito (no. 13670949)].

References

1. Wasnich RD, Paul D, Miller PD (2000) Antifracture efficacy of antiresorptive agents are related to changes in bone density. J Clin Endocrinol Metab 85:231–236

2. Reginster J-Y, Minne HW, Sorensen OH, Hooper M, Roux C, Brandi ML, Lund B, Ethgen D, Pack S, Roumagnac I, Eastell R (2000) Randomized trial of the effects of risedronate on vertebral fractures in women with established postmenopausal osteoporosis. Osteoporos Int 11:83–91
[SpringerLink] [ChemPort] [PubMed]

3. Borah B, Dufrensne TE, Chmielewski PA, Gross GJ, Prenger MC, Phipps RJ (2002) Risedronate preserves trabecular architecture and increases bone strength in vertebra of ovariectomized minipigs as measured by three-dimensional microcomputed tomography. J Bone Miner Res 17:1139–1147
[ChemPort] [PubMed]

4. Parfitt AM (1992) Implications of architecture for the pathogenesis and prevention of vertebral fracture. Bone 13:S41–S47
[crossref]

5. Ruegsegger P, Koller B, Mueller R (1996) A microtomographic system for the non-destructive evaluation of bone architecture. Calcif Tissue Int 58:24–29
[SpringerLink] ChemPort PubMed

6. Mueller R, Hahn M, Vogel M, Delling G, Ruegsegger P (1996) Morphometric analysis of non-invasively assessed bone biopsies: comparison of high-resolution computed tomography and histologic sections. Bone 18:215–220
crossref PubMed

7. Ito M, Nishida A, Nakamura T, Uetani M, Hayashi K (2002) Differences of three-dimensional trabecular microstructure in osteopenic rat models caused by ovariectomy and neurectomy. Bone 30:594–598
crossref ChemPort PubMed

8. Ito M, Nakamura T, Matsumoto T, Tsurusaki K, Hayashi K (1998) Analysis of trabecular microarchitecture of human iliac bone using microcomputed tomography in patients with hip arthrosis with or without vertebral fracture. Bone 23:163–169
crossref

9. Hildebrand T, Ruegsegger P (1997) A new method for the model-independent assessment of thickness in three-dimensional images. J Microsc 185:67–75
crossref

10. Laib A, Hildebrand T, Hauselmann HJ, Ruegsegger P (1997) Ridge number density: a new parameter for in vivo bone structure analysis. Bone 21:541–546
crossref ChemPort PubMed

11. Hildebrand T, Ruegsegger P (1997) Quantification of bone microarchitecture with the structure model index. Comput Methods Biomech Biomed Engin 1:15–23

12. Ulrich D, van Rietbergen B, Laib A, Ruegsegger P (1999) The ability of three-dimensional structural indices to reflect mechanical aspects of trabecular bone. Bone 25:55–60
crossref ChemPort PubMed

13. Boyce RW, Ebert DC, Youngs TA, Paddock CL, Mosekilde L, Stevens ML, Gundersen HJ (1995) Unbiased estimation of vertebral trabecular connectivity in calcium-restricted ovariectomized minipigs. Bone 16:637–642
crossref

14. Odgaard A, Gundersen HJ (1993) Quantification of connectivity in cancellous bone, with special emphasis on 3-D reconstructions. Bone 14:173–182
ChemPort PubMed

15. van Rietbergen B, Weinans H, Huiskes R, Odgaard A (1995) A new method to determine trabecular bone elastic properties and loading using micromechanical finite-element models. J Biomech 28:69–81
PubMed

16. van Rietbergen B, Huiskes R, Weinans H, Odgaard A, Kabel J (1995) The role of trabecular architecture in the anisotropic mechanical properties of bone. In: Odgaard A, Weinans H (eds) Bone structure and remodeling, World Scientific, Singapore, pp 137–145

17. van Rietbergen B, Odgaard A, Kabel J, Huiskes R (1996) Direct mechanics assessment of elastic symmetries and properties of trabecular bone architecture. J Biomech 29:1653–1657
crossref

18. Ito M, Nishida A, Nakamura T, Uetani M, Hayashi K (2002) Differences of three-dimensional trabecular microstructure in osteopenic rat models caused by ovariectomy and neurectomy. Bone 30:594–598

CrossRef ChemPort PubMed

19. Boyce RW, Paddock CL, Gleaso JR, Sletsema WK, Eriksen EF (1995) The effects of risedronate on canine cancellous bone remodeling: three-dimensional kinetic reconstruction of the remodeling site. J Bone Miner Res 10:211–221
ChemPort PubMed

20. Lin JH (1996) Bisphosphonates: a review of their pharmacokinetic properties. Bone 18:75–85
CrossRef ChemPort PubMed

21. Roschger P, Rinnerthaler S, Yates J, Rodan GA, Fratzl P, Klaushofer K (2001) Alendronate increases degree and uniformity of mineralization in cancellous bone and decreases the porosity in cortical bone of osteoporotic women. Bone 29:185–191
CrossRef

J Bone Miner Metab (2004) 22:335–340
DOI 10.1007/s00774-003-0491-x

Journal of
Bone and
Mineral
Metabolism

Effect of etidronate on three-dimensional trabecular structure in ovariectomized or sciatic neurectomized rats

Akifumi Nishida[1], Masako Ito[1], Masataka Uetani[1], Tatsuo Nakayama[2], and Tomoyuki Tanaka[2]

[1] Division of Radiological Science, Department of Radiology and Radiation Biology, Nagasaki University Graduate School of Biomedical Sciences, 1-7-1 Sakamoto, Nagasaki 852-8501, Japan
[2] Sumitomo Pharmaceuticals Research Division, Osaka, Japan

Abstract The purpose of this study was to evaluate the effect of etidronate (EHDP) on three-dimensional (3D) trabecular structure in ovariectomized (OVX) and sciatic neurectomized (NX) rats. Eight-week-old female Lewis rats received ovariectomy (n = 19) or sham operation (OVX-sham; n = 10). OVX rats received either vehicle (OVX-control; n = 9) or EHDP (OVX-EHDP; n = 10). Eight-week-old female Lewis rats received NX (n = 20) or sham operation (NX-sham; n = 10). NX rats received either vehicle (NX-control; n = 10) or EHDP (NX-EHDP; n = 10). EHDP at 5 mg/kg or vehicle was subcutaneously injected 5 days a week. The treatment was initiated 2 weeks after surgery and was continued for 2 weeks. At 12 weeks of age, the rats were killed, and we scanned the proximal metaphysis of the tibia; this was done using micro-CT; (μ CT20; SCANCO Medical). The recovery of structural parameters was not complete in NX rats compared to OVX rats. The 3D micro-CT images showed that the subcortical spongiosa, which was preserved in OVX rats, had marked loss in NX rats. Furthermore, these trabeculae were not restored after the EHDP treatment. In conclusion, the mechanical driving of the control of trabecular structure is inactive in NX, and EHDP treatment for 2 weeks does not restore this condition.

Key words micro-CT · three-dimensional (3D) · ovariectomy · immobilization · etidronate

Introduction

Both sex hormone and mechanical loading play an important role in the bone remodeling process. Ovariectomized (OVX) and sciatic neurectomized (NX) rats are osteopenic models of estrogen deficiency and immobilization, respectively. Although bone loss always accompanies trabecular deterioration, the degree or fashion of the deterioration may vary according to the osteopenic model. As both OVX and NX induce acceleration of bone resorption [1–6], the bisphosphonate, etidronate (EHDP) is expected to restore bone loss in these two conditions. Because the mechanism of bone loss is different between OVX and NX [5], the effect of EHDP is presumed to vary between them. The purpose of this study was to evaluate the effect of EHDP on the tree-dimensional (3D) trabecular structure in the two different osteopenic models, OVX and NX rats.

Offprint requests to: A. Nishida
(e-mail: d300039c@stcc.nagasaki-u.ac.jp)
Received: March 31, 2003 / Accepted: November 20, 2003

Materials and methods

Animals

Seven-week-old female Lewis rats were purchased from Charles River Japan (Yokohama, Japan) and acclimated under standard laboratory conditions at 23 ± 2°C and 50 ± 10% humidity. Rats were maintained in sterilized cages, fed standard rodent chow containing 1.25% Ca and 1.06% phosphate (CE-2; CLEA Japan, Tokyo, Japan), and allowed free access to tap water. Rats were allowed to acclimate for 1 week before the experiment.

Experimental design

OVX animals

A total of 29 female Lewis rats (8 weeks old) received ovariectomy (n = 19) or sham operation (OVX-sham; n = 10). Under pentobarbital anesthesia, rats were bilaterally ovariectomized. The success of the ovariectomy was confirmed by inspecting atrophy of the uterus. Ovariectomized rats were further divided into groups, receiving either vehicle (OVX-control; n = 9) or EHDP (OVX-EHDP; n = 10).

NX animals

A total of 30 female Lewis rats (8 weeks old) received unilateral left sciatic neurectomy (n = 20) or sham operation (NX-sham; n = 10) (these operations were described previously in more detail [5]). Neurectomized rats were further divided into groups, receiving either vehicle (NX-control; n = 10) or EHDP (NX-EHDP; n = 10).

EHDP at 5 mg/kg, or vehicle, was subcutaneously injected 5 days a week. The treatment was initiated 2 weeks after surgery and was continued for 2 weeks. Vehicle injections were given to sham and control groups under the same protocol. EHDP was synthesized at Sumitomo Pharmaceuticals (Osaka, Japan). The dose of EHDP was determined based on results of a previous study [6]. At 12 weeks of age, the rats were killed, the left tibiae were sampled, isolated from the surrounding soft tissue, and frozen at −40°C.

Data for some animals (OVX-sham, OVX-control, NX-sham, and NX-control rats) has been previously reported; in which we showed differences in the change of trabecular structure induced by OVX or NX [5].

Micro-computed tomography (CT)

The micro-CT apparatus (μ CT20) and the software used for analysis in this study were provided by SCANCO Medical (Basserdorf, Switzerland). The details of this micro-CT scanner have been previously described [7]. In short, the unit has a micro X-ray source (10 μm; 25 keV) directed toward the sample. After traversing the sample the X-rays are detected by a 1024-element charge-coupled device (CCD) array. The process is piloted by a DEC α-station (Digital Equipment, Marseille, France), and an OpenVMS system in cluster configuration to perform the 3D analysis. The proximal metaphysis of the tibia was scanned craniocaudally, including the border between the growth plate and bone, for 150 slices with 13-μm increments. The region of interest of 50 slices below the most distal part of the growth plate-metaphyseal junction was defined as the proximal portion, and 50 slices below the proximal portion was defined as the distal portion. The trabecular structure in the proximal portion and that in the distal portion were analyzed separately. The primary spongiosa may not have been excluded from the analyzed region, because it is impossible to clearly discriminate the primary spongiosa from secondary spongiosa in axial CT images. To obtain the original 3D image, a threshold value of 220 was chosen in this analysis system.

Morphometric and nonmetric parameters

On the original 3D image, morphometric indices were determined directly from the binalized volume of interest (VOI). The micro-CT allows a nominal resolution smaller than the thickness of trabeculae, and supplies a pixel size estimated at approximately 13 μm and a spatial resolution of 23 μm.

Bone surface area (BS) is calculated using the Marching Cubes method to triangulate the surface of the mineralized bone phase. Bone volume (BV) is calculated using tetrahedrons corresponding to the enclosed volume of the triangulated surface. Total volume (TV) is the volume of the whole examined sample. BV is normalized with TV to obtain the relative bone volume (BV/TV). Mean trabecular thickness (Tb.Th) was determined from the local thickness at each voxel representing bone. With this technique, thickness can be estimated without a model assumption [8]. Trabecular separation (Tb.Sp) was calculated by applying the same technique as that used for the direct thickness calculation to the non-bone parts of the 3D image. The trabecular number (Tb.N) was calculated by taking the inverse of the mean distance between the middle axes of the trabeculae. The structure model index (SMI) is a parameter recently proposed to provide an estimate of plate-rod characteristics of the structure [9]. The geometrical degree of anisotropy (DA) was defined from the ratio between the maximal and minimal radii of the mean intercept length (MIL) ellipsoid [10]. The MIL distribution was calculated by superimposing parallel test lines in different directions on the 3D image, where MIL denotes the mean distance between the bone/marrow interfaces. The MIL ellipsoid was calculated by fitting the MIL values to a directed ellipsoid. At ratios close to 1, the axes are of similar value and the bone structure is isotropic (structures in which trabeculae are similarly oriented). As the ratio increases above 1, the DA of the bone increases (structures in which trabeculae are not uniformly oriented). The trabecular bone pattern factor (TBPf), a parameter giving the ratio of concave to convex surfaces in 2D sections of trabeculae, was measured for each slice, and the mean value was determined for each specimen [11].

Statistical analysis

Comparisons of microstructural parameters between two groups were assessed by Student's t-test. The data values were presented as means ± SDs, and a P value of less than 0.05 was considered significant. Statistical analyses were performed with the Stat View software package (Stat View 5.0; Abacus Concepts, Berkeley, CA, USA)

Table 1. Body weights (g) of OVX-sham, OVX-control, OVX-EHDP, NX-sham, NX-control, and NX-EHDP groups

Group	Baseline	Week 2	Week 4
OVX-sham	169.3 ± 5.9	185.7 ± 7.7	197.6 ± 5.3
OVX-control	164.8 ± 6.1	206.6 ± 6.1*	229.4 ± 4.2*
OVX-EHDP	169.7 ± 5.4	206.4 ± 5.3*	229.0 ± 8.5*
NX-sham	173.6 ± 6.6	196.6 ± 9.9	204.5 ± 8.0
NX-control	177.8 ± 5.6	196.7 ± 6.7	200.9 ± 7.1
NX-EHDP	177.6 ± 6.1	196.8 ± 8.1	200.3 ± 9.0

* $P < 0.05$, compared with OVX-sham
Values are means ± SDs
OVX-sham, sham-operated and injected with vehicle; OVX-control, ovariectomized and injected with vehicle; OVX-EHDP, ovariectomized and injected with etidronate (EHDP); NX-sham, sham-operated and injected with vehicle; NX-control, sciatic neurectomized and injected with vehicle; NX-EHDP, sciatic neurectomized and injected with EHDP
There were no significant differences between NX-sham and NX-control or NX-EHDP

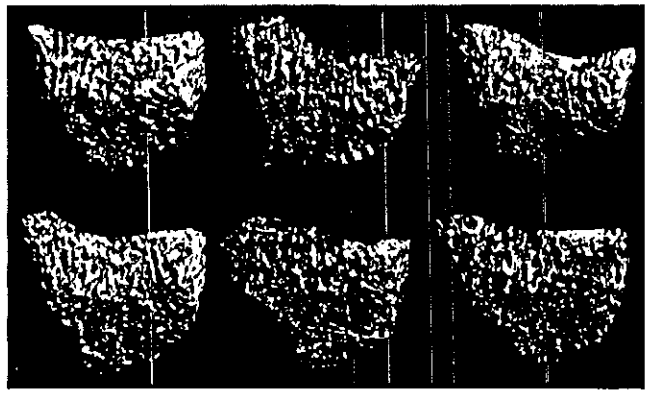

Fig. 1. Three-dimensional micro-CT images of the OVX-sham (upper left), OVX-control (upper middle), OVX-EHDP (upper right), NX-sham (lower left), NX-control (lower middle), and NX-EHDP (lower right)

Results

Body weight

Table 1 shows the changes in body weight. Body weight during the experimental period varied among the groups, but in all, it increased.

3D micro-CT images

Figure 1 demonstrates representative features of the 3D images of the trabecular structure of the OVX-sham (upper left), OVX-control (upper middle), OVX-EHDP (upper right), NX-sham (lower left), NX-control (lower middle), and NX-EHDP (lower right). The 3D images of the OVX-control and NX-control show significant bone loss. They clearly demonstrate that the trabeculae in the core portion of spongiosa show marked losts, and the trabeculae near the endocortical surface are relatively preserved in the OVX-control. In contrast, the trabeculae were diffusely lost in the NX-control. The 3D images of the OVX-EHDP and NX-EHDP demonstrate that EHDP treatment effectively prevented the bone loss; however, the respective characteristic trabecular distribution patterns of the OVX-control and the NX-control persisted even after the treatment.

Structural parameters

The structural parameters of OVX and NX rats are shown in Table 2 and Table 3, respectively.

OVX rat groups (Table 2)

In the proximal portion, 4 weeks after OVX, BV/TV was significantly reduced (−62%), associated with a significant decrease in Tb.N (−32%) and Tb.Th (−20%), and a significant increase in Tb.Sp (+46%), DA (+8%), SMI (+36%), and TBPf (+531%) in comparison with the OVX-sham. With the administration of EHDP, BV/TV was significantly increased (+205%), associated with a significant increase in Tb.N (+58%) and Tb.Th (+26%), and a significant decrease in Tb.Sp (−34%), DA (−9%), SMI (−39%) and TBPf (−115%) in comparison with the OVX-control.

In the distal portion, 4 weeks after OVX, BV/TV was significantly reduced (−64%), associated with significant decrease in Tb.N (−33%) and Tb.Th (−17%), and a significant increase in Tb.Sp (+51%), DA (+5%), SMI (+22%), and TBPf (+117%) in comparison with the OVX-sham. With the administration of EHDP, BV/TV was significantly increased (+80%), associated with a significant increase in Tb.N (+20%) and Tb.Th (+9%), and a significant decrease in Tb.Sp (−16%), SMI (−7%), and TBPf (−35%) in comparison with the OVX-control.

NX rat groups (Table 3)

In the proximal portion, 4 weeks after NX, BV/TV was significantly reduced (−83%) associated with a significant decrease in Tb.N (−47%) and Tb.Th (−38%) and a significant increase in Tb.Sp (+85%), SMI (+138%), and TBPf (+561%) in comparison with the NX-sham. With the administration of EHDP, BV/TV was significantly increased (+368%), associated with a significant increase in Tb.N (+55%) and Tb.Th (+60%), and a significant decrease in Tb.Sp (−28%), DA (−4%), SMI (−30%), and TBPf (−99%) in comparison with the NX-control.

In the distal portion, 4 weeks after NX, BV/TV was significantly reduced (−79%), associated with a significant decrease in Tb.N (−43%) and Tb.Th (−27%) and

Table 2. Comparison of morphometric and nonmetric parameters among OVX rat groups

Portion	Groups	Parameters						
		BV/TV	Tb.N	Tb.Th	Tb.Sp	DA	SMI	TBPf
Proximal	OVX-sham	0.256 ± 0.054	6.716 ± 0.268	0.066 ± 0.001	0.158 ± 0.006	1.190 ± 0.047	2.599 ± 0.456	2.199 ± 1.156
	OVX-control	0.095 ± 0.016*	4.54 ± 0.426*	0.053 ± 0.003*	0.231 ± 0.017*	1.286 ± 0.041*	3.543 ± 0.150*	13.875 ± 1.741*
	OVX-EHDP	0.290 ± 0.038**	7.153 ± 0.381**	0.067 ± 0.004**	0.153 ± 0.009**	1.171 ± 0.046**	2.146 ± 0.388**	−2.135 ± 2.535**
Distal	OVX-sham	0.198 ± 0.044	5.630 ± 0.618	0.066 ± 0.003	0.181 ± 0.018	1.258 ± 0.030	2.965 ± 0.326	7.444 ± 2.622
	OVX-control	0.071 ± 0.015*	3.788 ± 0.316*	0.055 ± 0.002*	0.274 ± 0.022*	1.350 ± 0.067*	3.611 ± 0.143*	16.142 ± 1.542*
	OVX-EHDP	0.128 ± 0.023**	4.555 ± 0.350**	0.060 ± 0.002**	0.231 ± 0.018**	1.301 ± 0.059	3.356 ± 0.168**	10.451 ± 1.523**

* $P < 0.05$, compared with OVX-sham; ** $P < 0.05$, compared with OVX-control
Values are means ± SDs
BV/TV, bone volume fraction; Tb.N, trabecular number; Tb.Th, trabecular thickness; Tb.Sp, trabecular separation; DA, degree of anisotropy; SMI, structure model index; TBPf, trabecular bone pattern factor; OVX-sham, sham-operated and injected with vehicle; OVX-control, ovariectomized and injected with vehicle; OVX-EHDP, ovariectomized and injected with EHDP

Table 3. Comparison of morphometric and nonmetric parameters among NX rat groups

Portion	Groups	Parameters						
		BV/TV	Tb.N	Tb.Th	Tb.Sp	DA	SMI	TBPf
Proximal	NX-sham	0.360 ± 0.100	7.931 ± 0.784	0.072 ± 0.015	0.132 ± 0.015	1.211 ± 0.033	1.624 ± 0.955	−4.127 ± 5.094
	NX-control	0.060 ± 0.017*	4.208 ± 0.418*	0.045 ± 0.002*	0.244 ± 0.025*	1.170 ± 0.059	3.863 ± 0.124*	19.040 ± 2.003*
	NX-EHDP	0.281 ± 0.112**	6.522 ± 1.682**	0.072 ± 0.034**	0.175 ± 0.046**	1.124 ± 0.027**	2.520 ± 0.808**	0.114 ± 7.719**
Distal	NX-sham	0.269 ± 0.060	6.515 ± 0.593	0.070 ± 0.005	0.156 ± 0.014	1.360 ± 0.063	2.465 ± 0.420	3.450 ± 3.444
	NX-control	0.056 ± 0.018*	3.698 ± 0.333*	0.051 ± 0.004*	0.278 ± 0.028*	1.254 ± 0.093*	3.819 ± 0.151*	18.382 ± 2.066*
	NX-EHDP	0.093 ± 0.031**	4.348 ± 0.555**	0.057 ± 0.005**	0.241 ± 0.030**	1.228 ± 0.058	3.766 ± 0.160	14.306 ± 3.297**

* $P < 0.05$, compared with NX-sham; ** $P < 0.05$, compared with NX-control
Values are means ± SDs
BV/TV, bone volume fraction; Tb.N, trabecular number; Tb.Th, trabecular thickness; Tb.Sp, trabecular separation; DA, degree of anisotropy; SMI, structure model index; TBPf, trabecular bone pattern factor; NX-sham, sham-operated and injected with vehicle; NX-control, sciatic neurectomized and injected with vehicle; NX-EHDP, sciatic neurectomized and injected with EHDP

DA (−8%) and a significant increase in Tb.Sp (+78%), SMI (+55%), and TBPf (+433%) in comparison with the NX-sham. With the administration of EHDP, BV/TV was significantly increased (+66%), associated with a significant increase in Tb.N (18%) and Tb.Th (+12%), and a significant decrease in Tb.Sp (−13%) and TBPf (−22%) in comparison with the NX-control.

Discussion

The objective of this study was to evaluate the effect of EHDP on 3D trabecular structure in OVX and NX rats. We used micro-CT, which provides 3D analysis of the trabecular structure. Because therapeutic administration is considered to be more important than preventive administration from the standpoint of the clinical treatment of osteoporosis, this study was designed as a therapeutic experiment. Previous studies indicated that OVX as well as NX induced rapid bone loss in rats, and significant bone loss was observed within 2 weeks [12,13]. Therefore we started treatment from 2 weeks after the operation to evaluate the therapeutic effect of EHDP.

The 3D micro-CT images clearly demonstrated the difference in trabecular distribution pattern between the OVX-control and the NX-control. The 3D image of the OVX-control showed marked bone loss in the core portion, while that of the NX-control showed diffuse bone loss. Similar findings in OVX and hindlimb-bandage rats have been reported using histomorphometry and scanning electron microscopy [14,15]. In these studies [14,15] the metaphysis was divided into three anatomical regions (lateral, central, and medial), and it was found that the loss of cancellous bone mass in the immobilization group was more uniform compared with that in the OVX group; the central zone in the immobilization group had 47.7% less bone mass than the medial zone compared with 71.8% less bone in the OVX group. The lateral and medial regions of the metaphysis have more mechanical loading, because this region transmits the forces and loads from the epiphysis and the growth plate to the diaphyseal cortex. It is suggested that bone resorption in the subcortical spongiosa was prevented by mechanical stress in the OVX-control. The 2-week treatment with EHDP obviously prevented the progression of bone loss; however, it did not change the characteristic trabecular distribution patterns that were shown in the OVX-control and the NX-control, respectively.

The micro-CT quantified the changes of structural parameters following EHDP treatment. EHDP increased BV/TV in relation to the increase in both Tb.Th and Tb.N. The recoveries of structural parameters were not complete in NX compared to OVX. This finding may be explained by the fact that both bone formation and bone resorption increase in OVX, while bone formation decreases and bone resorption increases in NX [1–4]. Bisphosphonates have been found to increase bone mass and to alleviate the trabecular deterioration in OVX and immobilization animals [3,4,6]. However, most of these studies used standard histomorphometry, which provides only 2D information about trabecular structure. A few studies have reported the effect of other bisphosphonates on 3D trabecular structure. Borah et al. [16] reported that risedronate prevented the deterioration of trabecular architecture in the vertebrae of OVX minipigs. Barou et al. [17] assessed the effect of tiludronate on tail-suspended rats, and reported that tiludronate restored the bone loss, mainly due to an increase of Tb.N. In the present study, 3D analysis provided additional direct information on anisotropy, which describes the extent to which the trabecular struts are aligned in a single direction (anisotropic) versus being randomly aligned (isotropic). We found a contrasting phenomenon, that OVX increased the DA while NX decreased it. It is suggested that OVX predominantly lose transverse trabeculae, inducing the structure to become anisotropic, while NX randomly lose trabeculae, inducing the structure to become isotropic. The EHDP treatment decreased the DA in the proximal portion in both OVX and NX rats, which indicates that EHDP treatment increases both the vertical and transverse trabeculae, inducing the structure to become more isotropic than those of the respective control groups. Because the DA is largely governed by the mechanical loading environment, it is suggested that the mechanical driving that controls trabecular structure is active in OVX, while it is inactive in NX.

We found that the effect of EHDP was stronger in the proximal portion than in the distal portion. The weaker effect in the distal portion was probably due to the more severe osteopenia in this portion. It is known that a sclerotic band is observed in the metaphysis on treatment with bisphosphonate in growing animals. Although the proximal portion may show the influence of a sclerotic band, the 3D micro-CT image showed no sclerotic band.

The bone volume of NX-sham rats was larger than that of the OVX-sham. We cannot provide a reason for this difference. As a speculation, it is possible that the difference in body weight at baseline, or the damage caused by the operations may have had some influence on causing the difference.

This study has a few shortcomings. Firstly, no rats were killed 2 weeks after the OVX or NX operation to evaluate bone loss at the start of the treatment. Secondly, there was no positive control group to compare EHDP with other currently available bisphosphonates. Thirdly, the treatment period of 2 weeks may be too short to evaluate the effect of EHDP on trabecular

structure. An additional study of longer treatment would be helpful to evaluate the full extent of the EHDP effect.

In conclusion, the recoveries of structural parameters by 2 weeks' treatment with EHDP were not complete in NX rats compared to OVX rats. Three-dimensional micro-CT images showed that the subcortical spongiosa, which was preserved in OVX rats, had marked loss in NX rats, and was not fully restored after the treatment. This finding suggests that the mechanical driving of the control of trabecular structure is inactive in NX, and EHDP treatment for 2 weeks does not restore this condition.

References

1. Zeng QQ, Jee WSS, Bigornia AE, King JG Jr, D'Souza SM, Li XJ, Ma YF, Wechter WJ (1996) Time responses of cancellous and cortical bones to sciatic neurectomy in growing female rats. Bone 19:13–21
2. Iwasaki Y, Yamato H, Murayama H, Sato M, Takahashi T, Ezawa I, Kurokawa K, Fukagawa M (2002) Maintenance of trabecular structure and bone volume by vitamin K2 in mature rats with long-term tail suspension. J Bone Miner Metab 20:216–222
3. Kodama Y, Nakayama K, Fuse H, Fukumoto S, Kawahara H, Takahashi H, Kurokawa T, Sekiguchi C, Nakamura T, Matsumoto T (1997) Inhibition of bone resorption by pamidronate cannot restore normal gain in cortical bone mass and strength in tail-suspended rapidly growing rats. J Bone Miner Res 12:1058–1067
4. Mosekilde L, Thomsen JS, Mackey MS, Phipps RJ (2000) Treatment with risedronate or alendronate prevents hindlimb immobilization-induced loss of bone density and strength in adult female rats. Bone 27:639–645
5. Ito M, Nishida A, Nakamura T, Uetani M, Hayashi K (2002) Differences of three-dimensional trabecular microstructure in osteopenic rat models caused by ovariectomy and neurectomy. Bone 30:594–598
6. Katsumata T, Nakamura T, Ohnishi H, Sakurama T (1995) Intermittent cyclical etidronate treatment maintains the mass, structure and the mechanical property of bone in ovariectomized rats. J Bone Miner Res 10:921–931
7. Ruegsegger P, Koller B, Mueller R (1996) A microtomographic system for the non-destructive evaluation of bone architecture. Calcif Tissue Int 58:24–29
8. Hildebrand T, Ruegsegger P (1997) A new method for the model independent assessment of thickness in three-dimensional images. J Microsc 185:67–75
9. Hildebrand T, Ruegsegger P (1997) Quantification of bone microarchitecture with the structure model index. Comput Methods Biomech Biomed Eng 1:15–23
10. Harrigan TP, Mann RW (1984) Characterization of microstructural anisotropy in orthopedic materials using a second rank tensor. J Mater Sci 19:761–767
11. Hahn M, Vogel M, Pompesius-Kempa M, Delling G (1992) Trabecular bone pattern factor—A new parameter for simple quantification of bone microarchitecture. Bone 13:327–330
12. Laib A, Kumer JL, Majumdar S, Lane NE (2001) The temporal changes of trabecular architecture in ovariectomized rats assessed by MicroCT. Osteoporosis Int 12:936–941
13. Laib A, Barou O, Vico L, Lafage-Proust MH, Alexandre C, Ruegsegger P (2000) 3D micro-computed tomography of trabecular and cortical bone architecture with application to a rat model of immobilization osteoporosis. Med Biol Eng Comput 38:326–332
14. Bagi CM, Miller SC (1994) Comparison of osteopenic changes in cancellous bone induced by ovariectomy and/or immobilization in adult rats. Anat Rec 239:243–254
15. Miller SC, Bowman BM (1998) Comparison of bone loss during normal lactation with estrogen deficiency osteopenia and immobilization osteopenia in rat. Anat Rec 251:265–274
16. Borah B, Dufresne TE, Chmielewski PA, Gross GJ, Prenger MC, Phipps RJ (2002) Risedronate preserves trabecular architecture and increases bone strength in vertebra of ovariectomized minipigs as measured by three-dimensional microcomputed tomography. J Bone Miner Res 17:1139–1147
17. Barou O, Lafage-Proust MH, Martel C, Thomas T, Tirode F, Laroche N, Barbier A, Alexandre C, Vico L (1999) Bisphosphonates effects in rat unloaded hindlimb bone loss model: three-dimensional microcomputed tomographic, histomorphometric, and densitometric analysis. J Pharmacol Exp Ther 291: 321–328

J Bone Miner Metab (2004) 22:404–414
DOI 10.1007/s00774-004-0502-6

Journal of
Bone and
Mineral
Metabolism

Original articles

Regulation of mineral-to-matrix ratio of lumbar trabecular bone in ovariectomized rats treated with risedronate in combination with or without vitamin K_2

HAJIME OTOMO[1], AKINORI SAKAI[1], SATOSHI IKEDA[1], SHINYA TANAKA[1], MASAKO ITO[2], ROGER J. PHIPPS[3], and TOSHITAKA NAKAMURA[1]

[1]Department of Orthopaedic Surgery, University of Occupational and Environmental Health, School of Medicine, 1-1 Iseigaoka, Yahatanishi-ku, Kitakyushu 807-8555, Japan
[2]Department of Radiology, Nagasaki University, Nagasaki, Japan
[3]Procter & Gamble Pharmaceuticals, Cincinnati, OH, USA

Abstract The relationship between bone turnover and bone tissue and material properties was examined in ovariectomized (OVX) rats treated with risedronate in combination with or without vitamin K_2. Seventy female rats, 18 weeks of age, were assigned to 7 groups (n = 10): sham-operated + vehicle control; OVX + vehicle control; OVX + risedronate 0.1, 0.5, or 2.5 mg/kg/day po; OVX + vitamin K_2 ~30 mg/kg/day po; OVX + vitamin K_2 (~30 mg/kg/day) and risedronate (0.5 mg/kg/day). Treatments were given daily for 9 months. To assess bone turnover, we measured serum osteocalcin and urinary deoxypyridinoline at 0, 3, and 9 months. To assess vertebral and femoral tissue and material properties, bone mass, bone mineral density (BMD by DXA), trabecular bone structure (vertebra: 3D-μCT), cortical bone structure (femur: histomorphometry), biomechanical properties, and mineral properties (mineral-to-matrix and carbonate-to-phosphate ratios by Fourier transform infrared microspectroscopy) were measured ex vivo at 9 months. Ovariectomy increased bone turnover and induced significant loss of bone mass/density, structure, mineral properties (mineral-to-matrix ratio), and strength. Risedronate produced dose-dependent inhibition of the ovariectomy-induced increase in turnover and loss of bone mass/density, structure, mineral-to-matrix ratio, and strength, with a lowest effective dose of 0.1–0.5 mg/kg/day. High-dose risedronate (2.5 mg/kg/day) did not induce increases in any parameter above that of sham control. Vitamin K_2 had no effects. In the OVX groups, urinary deoxypyridinoline at 3 and 9 months correlated significantly with vertebral BMD, trabecular bone volume, ultimate load, stiffness, and mineral-to-matrix ratio, and with femoral BMD, cortical area, and ultimate load. These results support the concept that changes in bone tissue and material properties can result directly from changes in bone turnover. Different effects among different drugs on material properties, including mineral-to-matrix ratio, may reflect differences in the relative rate and magnitude of osteoclastic bone resorption and osteoblastic primary bone mineralization.

Offprint requests to: H. Otomo
(e-mail: h-otomo@med.uoeh-u.ac.jp)
Received: December 15, 2003 / Accepted: February 27, 2004

Key words bisphosphonates · bone turnover markers · bone 3D micro-CT · bone mineral properties · ovariectomized rat

Introduction

Nitrogen-containing bisphosphonates such as alendronate and risedronate have emerged as standard therapeutic agents for treating postmenopausal osteoporosis [1,2]. These agents can prevent bone loss after cessation of ovarian function by reducing bone turnover. Bone mineral density (BMD) increases rapidly during the first year of treatment, by 3%–6%, followed by a smaller but progressive increase. The increase in BMD is associated with a reduction in the fracture risk [3–6]. Although antifracture efficacy of antiresorptive agents is related to changes in BMD [7,8], it is obvious that there are other confounding factors that contribute to the risk of vertebral fragility fractures, such as microarchitecture deterioration [9–13]. The reasons for the increase in BMD with antiresorptive drugs are not completely understood, although there is some evidence that an increase in mineralization at the tissue level occurs with bisphosphonates [14,15]. Because the various antiresorptive agents act to reduce bone turnover through different mechanisms [16], the relationships of bone turnover, mineralization, and fracture risk reduction may be different in patients with postmenopausal osteoporosis during treatment with different antiresorptive agents.

Recently, in addition to bone mechanical and structural properties, effects of bisphosphonates on mineral properties have been assessed in normal and in ovariectomized animals [17–19]. Administration of pamidronate for a year in dogs resulted in abnormal bone mineralization, including increased crystal size [17]. Daily ibandronate administration in ovariohysterectomized dogs for a year increased mineral-to-matrix

ratio and increased size and maturity of the hydroxyapatite crystals when activation frequency was depressed to below the level in sham-operated dogs [18]. Tiludronate administration for a year prevented changes in the chemical parameters of trabecular bone mineralization in ovariectomized rats [19]. These studies, using different methods to evaluate mineralization, consistently indicate that bisphosphonates can affect the mineral properties at the bone tissue level. Although increases in bone tissue mineralization by bisphosphonates are suggested to be due to the extended time period before the mineralized bone tissue can undergo resorption [14,15,20], the relationships of bone turnover and mineral and mechanical properties have not been well explored in ovariectomized animals treated with bisphosphonates.

We hypothesized that the change in bone turnover predicts the change in mechanical and mineral properties of bone in ovariectomized rats treated with bisphosphonates. For this purpose, we studied the effects of risedronate, in combination with or without vitamin K_2. Vitamin K_2 is known to be essential for the γ-carboxylation of osteocalcin, the major noncollagenous bone protein [21], activating osteoblasts to enhance mineralization in vitro [22]. The positive effects of vitamin K_2 on bone mass, strength, and structure have been previously demonstrated by various animal models [23–26]. The clinical efficacy of vitamin K_2 treatment for postmenopausal osteoporosis has also been reported [27–29]. We measured bone chemical markers as a surrogate of bone turnover, bone mineral by dual-energy X-ray absorptiometry (DXA), structure of the lumbar vertebral trabeculae by micro-computed tomography (micro-CT) and of the femoral cortex from histomorphometry in undecalcified sections, and the mineral properties of vertebra and femur by Fourier transform infrared (FTIR) microspectroscopy. We also performed biomechanical testing of the lumbar vertebra and femur. The relationships of bone chemical markers with bone mass, mechanical, and mineral parameters were analyzed.

Materials and methods

Experimental animals

Female Sprague-Dawley (SD) CD rats, 9 weeks of age, were purchased from Charles River Japan (Hino, Japan) and acclimated for 9 weeks before the experiment. The rats had free access to water using an automatic water supply apparatus (Edstrom, Waterford, WI, USA) and commercial standard rodent chow (CE-2) containing 1.25% calcium, 1.06% phosphate, and 2.0 IU/g vitamin D_3 (Clea Japan, Tokyo, Japan) during the acclimation period. All animals were fasted between approximately 4 h before administration and approximately 2 h after administration of risedronate daily. Each rat was housed in a stainless steel cage in an air-conditioned environment (room temperature 22° ± 2°C, humidity 50% ± 10%) illuminated from 600 to 1800. Body weight and food consumption were measured once a week.

Experimental protocol

Seventy rats, at the age of 18 weeks, were randomly assigned to 7 groups by body weight (BW) (Table 1). The rats underwent sham surgery (sham) in one group (group 1) and bilateral ovariectomy (OVX) in the other six groups (groups 2–7) by a dorsal approach under ether anesthesia. Risedronate was administered orally via a catheter at 0.1, 0.5, and 2.5 mg/kg BW once daily for 9 consecutive months (groups 3–5, 7). These doses are described as low (0.1), mid (0.5), and high (2.5) doses of risedronate. Animals of the vehicle group were dosed orally with physiological saline in the same manner. Vitamin K_2 was administered orally mixed with food at approximately 30 mg/kg BW per day as a dietary supplement for 9 consecutive months (groups 6, 7). Thus, group 6 received vitamin K_2 alone, and group 7 received the combination of risedronate (0.5 mg/kg/day) and vitamin K_2. Vitamin K_2 was weighed and mixed thoroughly with food (CE-2) to ensure homogeneity.

Table 1. Study design

Group	*n*	Surgical treatment	Test article[a]	Dosage (mg/kg/day)	Dose volume (ml/kg/day)
1	10	Sham[b]	Vehicle	0	10
2	9[c]	OVX	Vehicle	0	10
3	10	OVX	Risedronate	0.1	10
4	10	OVX	Risedronate	0.5	10
5	10	OVX	Risedronate	2.5	10
6	10	OVX	Vehicle + vitamin K_2	0 + 30	10 + ad libitum
7	10	OVX	Risedronate + vitamin K_2	0.5 + 30	10 + ad libitum

[a] Risedronate and vehicle (physiological saline) administered orally by gavage; vitamin K_2 administered orally in feed
[b] Animals of group 1 were not ovariectomized (OVX)
[c] One animal was excluded

The following formula was used for mixing vitamin K_2 with food: content of vitamin K_2 in food (mg/g) = [mean body weight (kg) × dose level (mg/kg/day)] / [average food consumption per each animal (g/day)].

Urine samples (24-h) were collected from each rat in group 1 once at baseline and at 3 and 9 months after the initiation of dosing in all groups. Blood samples were collected from the jugular vein at baseline, at 3 months, and at termination (9 months), and were centrifuged to obtain serum. After exsanguination under ether anesthesia, the fourth and fifth lumbar vertebrae (L4, L5) and both femurs were removed. Urine and serum samples were collected and were stored at −20°C until assay. The right femur and L4 vertebra were stored at −80°C until biomechanical testing. The left femur and L5 vertebra were stored in 70% ethanol solution for bone mineral analysis (by FTIR).

Bone metabolic markers

Serum osteocalcin levels were measured with a radioimmunoassay kit (Immutopics, San Clemente, CA, USA) using antirat osteocalcin antibody. Urinary deoxypyridinoline (DPD) levels were determined with an enzyme immunoassay kit (Osteolinks; Metra Biosystems, Mountain View, CA, USA). Urinary creatinine levels were measured by the autoanalyzer. DPD levels were corrected for urinary creatinine concentration.

Bone size and bone mineral measurement

The length of the right femur and the height of the L4 vertebral body were measured with a micrometer after adhering soft tissues had been trimmed away. The volume of the specimen was measured by the method of Archimedes using a volumetric apparatus (MK-550; Muromachi, Tokyo, Japan). Bone mineral density (BMD, mg/cm^2) of the right femur and the L4 vertebral specimens were measured by DXA (DCS-600EX-III R; Aloka, Tokyo, Japan) with irradiation applied anteroposteriorly to the specimen. Values of BMD for the whole L4 vertebral body and the middiaphyseal region of right femur were obtained.

Structural analysis using micro-CT

After the removal of adhering tissues, the posterior elements, and transverse processes of the L4 vertebral body, each specimen was scanned by micro-CT (μCT40; Scanco Medical, Bassersdorf, Switzerland). The whole L4 vertebral body was scanned dorsoventrally using 240 slices with 8-μm increments. In the three-dimensional (3D) analysis, the tissue volume (TV, mm^3) and the trabecular bone volume (BV, mm^3) were measured by the direct method available on the machine [30], and the trabecular bone volume fraction (BV/TV, %) was calculated. Trabecular thickness (Tb.Th, μm), trabecular separation (Tb.Sp, μm), and trabecular number (Tb.N, 1/mm) were measured directly on 3D images. Connectivity density (mm^{-3}) is a topological parameter that estimates the number of trabecular connections per cubic millimeter. The perforation of plates without the breaking of trabecular connections would artificially increase connectivity density [31]. Therefore, in our calculation, a stepwise dilation of the bone voxels was used to remove the holes, thereby minimizing the contribution from perforations. After a three-step dilation, connectivity density was derived from the Euler number [32].

Bone histomorphometry

An undecalcified section was obtained from the site of the middiaphisis of the left femur. The specimen was dehydrated and embedded in methylmethacrylate (MMA) without staining to yield a 20-μm-thick cross-cut ground section. The measurements were performed on the cathode ray tube (CRT) monitor with a charge-coupled device (CCD) camera (CCD High Gain Color Camera HCC-1600A; Flovel, Tokyo, Japan) setting on the microscope using the semiautomatic image analyzing program (Mac Scope; Mitani, Fukui, Japan) on a computer (Power Macintosh 7500/100). Total cross-sectional area (mm^2), bone marrow area (mm^2), and cortical bone area (mm^2) were obtained. The endocortical surface was approximated as a regular, continuous line. Moment of inertia (I, mm^4) of the cortical bone area for the mediolateral axis was calculated directly by the image-analyzing computer.

Mechanical tests

The L4 vertebral body was fixed with a clamp at the bases of the transverse processes in the holder of a diamond band saw (Exakt, Norderstedt, Germany). By removing both the cranial and caudal endplates, a central cylinder specimen with planoparallel end surfaces and a height of 3.6 mm was obtained for a compression test [33,34]. BMD and volumes of the L4 cylinder specimens were then obtained. The cylinder specimens were placed centrally on the smooth surface of a steel disk (10 cm diameter) attached to the materials testing machine (Tensilon UTA-1T; Orientec, Tokyo, Japan). A compression force was applied in a craniocaudal direction to the specimen with a steel disk (1.8 cm diameter) at a deformation rate of 2 mm/min. Crosshead displacement was considered as specimen deformation. Ultimate compressive load (N) and structural modulus (N/mm) were obtained directly from the load-deformation curve. The load values were corrected for the BMD and volume of the specimen.

Three-point bending test of the femur was performed using the same instrument (Tensilon UTA-1T; Orientec) [33,35]. The right femur specimen was placed on a special holding device with supports located at a distance of 13 mm (L). The bending force was applied with the cross head at a speed of 10 mm/min, until fracture occurred. Ultimate bending load (N) and structural modulus (N/mm) were obtained from the load-deformation curve. The material strength (Ms: normalized bending strength, N/mm^2) was calculated from the following equation: Ms = M/Z where M (the bending moment to failure, N·mm) = 1/4 × ultimate load (N) × L (mm), Z (the modulus of section, mm^3) = 2 × I/D, L (mm) is the distance between the supports of the holding device (13 mm), I (mm^4) is the moment of inertia, and D is the anteroposterior outer diameter (mm) [23].

FTIR microspectroscopic analysis

Mineral properties including mineral-to-matrix ratio and carbonate-to-phosphate ratio of trabecular bone of L5 vertebra and the middiaphyseal cortical bone of left femur were measured using FTIR microspectroscopy [19,36]. Bone samples were fixed and dehydrated in ethanol and embedded in MMA undecalcified. One 5-μm section was obtained from each L5 vertebra (midsagittal) and left femur (cross-cut area). In each L5 vertebral section, two areas about 100 μm in diameter from the midtrabecular region were measured under the optical microscope (Nikon SMZ-U). The bone-resorbing or bone-forming status of the trabecular bone surfaces was not taken into consideration in sampling. Sampled trabeculae were located in the center of metaphysis, 1 mm apart from the cranial and caudal growth plate, respectively. In each femur section, two areas were obtained from the midportion of the anterior and posterior cortices.

FTIR microspectroscopic data were recorded with a WINSPEC 50 spectrometer (Jeol, Tokyo, Japan) equipped with an IR-MAU 200 microscope (Jeol) fitted with a narrow-band MCT detector cooled to 77 K. A 20 × Reflachromat objective and condenser and a rectangular remote aperture were used for data acquisition. IR spectra were collected in the transmission mode, 100 scans per area, 4 cm^{-1} resolution. The sample was placed in the diamond cell. One measurement was performed for one sample, then the mean values of two samples were obtained for both L5 and femur sections. Individual bands in the 1800 to 800 cm^{-1} spectral region from infrared spectra acquired by FTIR microspectroscopy were baseline corrected. Subsequently, the ratio of mineral (PO_4, 1180–910 cm^{-1}) to matrix (amide I, 1590–1715 cm^{-1}), and carbonate (CO_3, 890–850 cm^{-1}) to phosphate (PO_4, 1180–910 cm^{-1}) were deduced from the ratio of the integrated areas of the respective raw peaks.

Statistical analysis

All data are expressed as the mean ± standard deviation of the mean (SD) for tables and mean ± standard error (SE) of mean for figures. To assess the effects of overiectomy in rats, the data of group 2 (OVX controls) were compared with the data of group 1 (sham, placebo controls) by Student's *t* test for homogeneous variances. If variances were not homogeneous, the Mann–Whitney *U* test was applied. The intergroup differences among OVX groups (groups 2–7) were evaluated by one-way analysis of variance (ANOVA) followed by Fisher's protected least squares difference (PLSD) test after the Bartlett test. The linear regression analyses were performed to assess the relationships between bone chemical markers and the parameters of bone mass and mechanical and mineral properties. A *P* value of less than 0.05 was considered significant. The analysis was performed using Stat View 5.0 software (Macintosh, Apple Computer, Cupertino, CA, USA).

Results

Body weight and vitamin K_2 intake

One rat in group 2 was excluded from measurement because of incomplete ovariectomy determined at necropsy. Body weights for groups 1–7 at the end of the treatment period were 368.0 ± 22.5, 443.1 ± 30.5, 438.0 ± 59.4, 437.4 ± 37.5, 411.6 ± 39.1, 426.3 ± 25.9, and 466.4 ± 46.8 g, respectively. The values in all OVX groups (groups 2–7) were significantly larger than the value in sham controls (group 1). The values did not significantly differ among the OVX groups. The mean vitamin K_2 intakes during the period in groups 6 and 7 were 29.85 ± 2.43 and 29.84 ± 1.77 mg/kg/day, respectively.

Serum osteocalcin and urinary DPD levels

Serum osteocalcin and urinary DPD levels were significantly increased by ovariectomy (group 2 *vs* group 1) at 3 and 9 months (Fig. 1A,B). Compared to OVX controls (group 2), serum osteocalcin in all treated groups (groups 3–7) was significantly reduced at 3 and 9 months. Urinary DPD levels were significantly reduced by mid-dose and high-dose risedronate (groups 4, 5, and 7) at 3 and 9 months. However, low-dose risedronate (group 3) and vitamin K_2 alone (group 6) did not alter the urinary DPD levels versus those in OVX controls (group 2) at either 3 or 9 months.

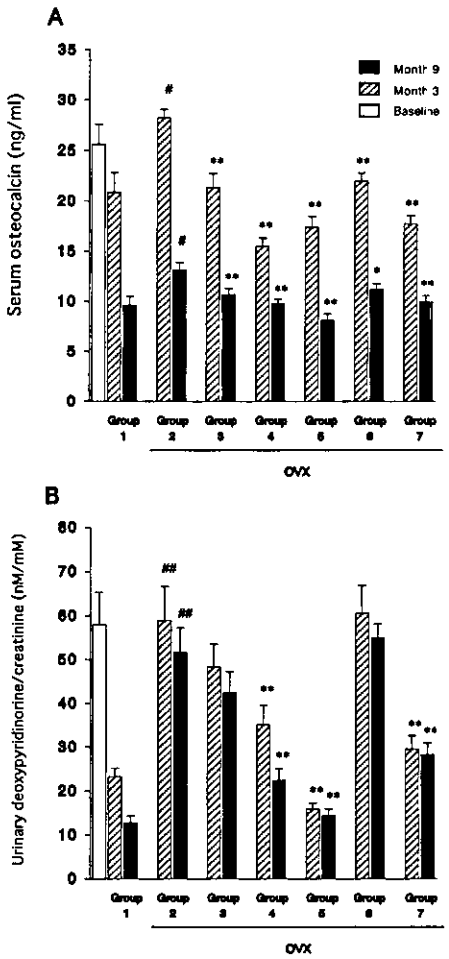

Fig. 1. Biochemical analysis of serum osteocalcin (**A**) and urinary deoxypyridinoline (DPD) (**B**) in rats at the start of the experiment and 3 and 9 months after surgery. Data are presented as the mean + SEM (n = 9 or 10). #$P < 0.05$, ##$P <$ 0.01 ovariectomized (OVX) control (group 2) vs sham control group (group 1) (Mann-Whitney U test). *$P < 0.05$, **$P <$ 0.01 vs treated groups (groups 3–7) vs OVX control (group 2) (ANOVA followed by Fisher's PLSD test after Bartlett test). Group 1, sham + vehicle; group 2, OVX + vehicle; group 3, OVX + risedronate 0.1 mg/kg/day; group 4, OVX + risedronate 0.5 mg/kg/day; group 5, OVX + risedronate 2.5 mg/kg/day; group 6, OVX + vehicle + vitamin K_2 30 mg/kg/day; group 7, OVX + risedronate 0.5 mg/kg/day + vitamin K_2 30 mg/kg/day

Bone size and BMD

Bone sizes and volumes of L4 vertebra and femur (taken at necropsy at 9 months) did not significantly differ among groups (Table 2). BMD of L4 vertebra and femur in OVX controls (group 2) were significantly smaller than the respective values in sham controls (group 1). Mid-dose and high-dose risedronate (groups 4, 5, and 7) significantly increased BMD of L4 vertebra and femur versus OVX controls (group 2). Low-dose risedronate (group 3) and vitamin K_2 alone (group 6) had no effect.

Parameters of bone structure

Lumbar vertebra: in OVX controls (group 2), BV/TV, Tb.N, and connectivity density were significantly lower and Tb.Sp was significantly larger in lumbar vertebral bone compared to sham controls (group 1) (Table 3). Mid-dose and high-dose risedronate (groups 4, 5, and 7) significantly increased BV/TV, Tb.N, and connectivity density and significantly reduced Tb.Sp versus OVX controls (group 2). With low-dose risedronate (group 3), Tb.Sp and Tb.Th were significantly reduced versus OVX controls (group 2).

Femur: total cross-sectional area, bone marrow area, and moment of inertia in the mid-femur did not significantly differ among groups. Cortical bone area was significantly increased in mid-dose and high-dose risedronate groups (groups 4, 5, and 7) versus OVX controls (group 2). Moment of inertia did not significantly differ among groups.

Bone mechanical properties

Lumbar vertebra: in OVX controls (group 2), ultimate compressive load and structural modulus of the lumbar vertebral bone were significantly lower than in sham controls (group 1) (Table 4). Mid-dose and high-dose risedronate (groups 4, 5, and 7) significantly increased ultimate load and structural modulus versus OVX controls (group 2). Vitamin K_2 alone (group 6) had no effect on lumbar vertebral biomechanical properties.

Femur: in OVX controls (group 2), ultimate bending load and structural modulus of femur were not significantly different from sham controls (group 2 *vs* group 1). Mid-dose and high-dose risedronate significantly increased ultimate bending load versus OVX controls (group 2). Material strength did not significantly differ among groups.

Mineralization properties

Lumbar vertebra: in OVX controls (group 2), mineral-to-matrix ratio (PO_4/amide I area ratio) in the trabecular bone was significantly lower than in sham controls (group 1) (Table 5). All dose levels of risedronate (groups 3, 4, 5, and 7) significantly increased mineral-to-matrix ratio versus OVX controls (group 2). Vitamin K_2 alone (group 6) had no effect. For carbonate-to-phosphate ratio (CO_3/PO_4 area ratio), there were no differences among groups.

Femur: there were no significant differences among groups in either mineral-to-matrix or carbonate-to-phosphonate ratios in the center of femoral cortices.

Table 2. Bone height or length, volume, and BMD of the fourth lumbar vertebra and the right midfemur in OVX rats treated with risedronate or vitamin K_2

Group	Height	Length	Volume		BMD	
	L4 (mm)	Right femur (mm)	L4 (mm^3)	Right femur (mm^3)	L4 (mg/cm^2)	Right femur (mg/cm^2)
1. Sham + vehicle	7.4 ± 0.38	37.9 ± 0.73	55.7 ± 5.4	697.3 ± 73.6	84.8 ± 5.5	178.6 ± 10.1
2. OVX + vehicle	7.4 ± 0.45	37.9 ± 0.94	52.3 ± 6.1	707.6 ± 46.5	67.6 ± 8.2*	166.2 ± 5.8*
3. OVX + risedronate 0.1 mg/kg/day	7.4 ± 0.34	37.6 ± 1.08	54.3 ± 6.9	698.4 ± 74.3	73.8 ± 8.4	172.5 ± 6.3
4. OVX + risedronate 0.5 mg/kg/day	7.4 ± 0.38	38.0 ± 1.02	55.1 ± 6.7	687.0 ± 52.7	79.5 ± 6.6**	184.2 ± 5.1**
5. OVX + risedronate 2.5 mg/kg/day	7.4 ± 0.45	37.6 ± 0.86	57.5 ± 6.3	702.7 ± 50.3	89.4 ± 5.5**	189.1 ± 9.8**
6. OVX + vehicle + vitamin K_2 30 mg/kg/day	7.5 ± 0.44	37.9 ± 0.93	56.2 ± 10.3	683.6 ± 67.1	72.1 ± 7.1	172.1 ± 8.6
7. OVX + risedronate 0.5 mg/kg/day + vitamin K_2 30 mg/kg/day	7.3 ± 0.37	37.9 ± 0.71	53.6 ± 6.7	701.6 ± 63.9	80.6 ± 5.0**	187.9 ± 11.5**

Data are presented as the mean ± SD (n = 9 or 10)
* $P < 0.01$ OVX control (group 2) vs sham control (group 1) (Student's t test); ** $P < 0.01$ treated groups (groups 3–7) vs OVX control (group 2) (ANOVA followed by Fisher's PLSD test after Bartlett test)

Correlation of urinary DPD and BMD, structure, and mechanical and mineralization properties of lumbar vertebra and femur

Lumbar vertebra: urinary DPD levels in groups 2–7 and groups 2–5 at 3 and 9 months significantly correlated with BMD, BV/TV, ultimate load, stiffness, and mineral-to-matrix ratio in the lumbar vertebra. They did not correlate with carbonate-to-phosphonate ratio (Table 6).

Femur: urinary DPD levels significantly correlated with BMD, cortical area, and ultimate load in femur. They did not correlate with stiffness and mineral properties.

Ultimate load and mineral-to-matrix ratio of lumbar vertebra showed high inverse correlations with urinary DPD values at 9 months in groups 1–7, with P values < 0.0001 (Fig. 2A,B).

Discussion

This study demonstrated that 9-month risedronate administration prevented the increase in bone turnover and the loss of mechanical and mineral properties in lumbar vertebral bone and femur induced by OVX in rats. Age-dependent increases in BMD, cross-sectional cortical bone structure, and ultimate bending load in femur, apparently reduced after OVX, were also maintained by risedronate. Administration of vitamin K_2 did not affect these parameters in OVX rats in this study.

Risedronate produced dose-related effects on the measured parameters of bone mass and quality. Effects of risedronate on BMD and the parameters of 3D trabecular bone structure of the lumbar vertebra in OVX rats were consistent with previous studies [37,38]. In this study, similar effects were seen at the mid and high doses of risedronate (0.5 and 2.5 mg/kg/day). Effects at the low dose (0.1 mg/kg/day) were less consistent. All doses prevented the increase in serum osteocalcin levels after OVX, while only the 0.5 and 2.5 mg/kg/day doses prevented the increase of urinary DPD levels. The preventive effects on BMD and mechanical properties were also significant from the dose of 0.5 mg/kg/day. However, the decrease in lumbar vertebral Tb.Sp and the decrease in the mineral-to-matrix ratio of the trabecular bone were prevented at all dose levels. Thus, it is reasonable to conclude that the regulation of bone turnover by risedronate prevented the deterioration of trabecular bone structure and the reduction in the mineral-to-matrix ratio of trabecular bone tissue in OVX rats at 0.1 mg/kg/day and higher doses. The results suggest that the mineral-to-matrix ratio of trabecular bone, serum osteocalcin, and 3D trabecular Tb.Sp of vertebra could be sensitive indices for effects on bone turnover in OVX rats treated with risedronate.

Mechanical properties of lumbar vertebra and femur at 9 months were inversely correlated with bone chemical markers at 3 and 9 months after the start of risedronate treatment. The mechanical parameters and other parameters of bone quality such as bone structure and mineral properties after treatment with 2.5 mg/kg/day risedronate were not different from those in sham-operated rats. Thus, the reduction in bone turnover by risedronate would not be expected to produce any deterioration in the bone quality or increase brittleness of bone in OVX rats due to hypermineralization of bone [39]. In humans, the reduction in bone resorption markers below the level of those seen in premenopausal

Table 3. Structural indices of the fourth lumbar vertebra and the right midfemur in OVX rats treated with risedronate or vitamin K_2

Group	Microarchitectural indices of L4 vertebra					Cross-sectional morphology of midfemoral cortex			
	BV/TV (%)	Tb.Th (μm)	Tb.Sp (μm)	Tb.N (/mm)	Connectivity density	Total cross-sectional area (mm^2)	Bone marrow area (mm^2)	Cortical bone area (mm^2)	Moment of inertia (mm^4)
1. Sham + vehicle	42.3 ± 4.7	68.9 ± 5.3	139.1 ± 25.7	8.0 ± 1.7	192.5 ± 56.9	9.4 ± 1.08	3.4 ± 0.50	6.0 ± 0.71	4.2 ± 1.11
2. OVX + vehicle	25.1 ± 6.1*	66.9 ± 3.3	249.2 ± 59.4*	4.5 ± 1.2*	88.6 ± 39.0*	9.6 ± 1.02	4.0 ± 0.85	5.7 ± 0.26	4.2 ± 0.99
3. OVX + risedronate 0.1 mg/kg/day	28.2 ± 6.0	62.9 ± 4.4**	208.4 ± 37.7**	5.1 ± 1.1	120.1 ± 50.0	9.4 ± 0.80	3.6 ± 0.45	5.8 ± 0.67	4.3 ± 0.96
4. OVX + risedronate 0.5 mg/kg/day	33.3 ± 4.5***	64.2 ± 3.5	163.6 ± 23.6***	6.4 ± 1.0***	154.6 ± 27.9**	9.8 ± 0.78	3.3 ± 0.54	6.5 ± 0.36***	4.8 ± 0.89
5. OVX + risedronate 2.5 mg/kg/day	41.1 ± 3.6***	66.1 ± 2.2	127.1 ± 18.2***	8.5 ± 1.3***	277.1 ± 101.2***	9.9 ± 0.68	3.6 ± 0.59	6.3 ± 0.32**	4.5 ± 0.44
6. OVX + vehicle + vitamin K_2 30 mg/kg/day	27.0 ± 5.7	68.6 ± 4.9	245.3 ± 56.4	4.5 ± 1.1	81.8 ± 29.1	9.6 ± 0.99	3.6 ± 0.71	5.9 ± 0.53	4.3 ± 0.86
7. OVX + risedronate 0.5 mg/kg/day + vitamin K_2 30 mg/kg/day	36.2 ± 6.3***	65.8 ± 4.4	159.6 ± 24.2***	6.7 ± 1.3***	190.0 ± 62.9***	10.0 ± 1.24	3.6 ± 0.75	6.4 ± 0.73***	4.8 ± 1.35

Data are presented as the mean ± SD (n = 9 or 10)
BV/TV, trabecular bone volume/tissue volume; Tb.Th, trabecular thickness; Tb.Sp, trabecular separation; Tb.N, trabecular number
* $P < 0.01$ OVX control (group 2) vs sham control (group 1) (Student's t test); ** $P < 0.05$, *** $P < 0.01$ treated groups (groups 3–7) vs OVX control (group 2) (ANOVA followed by Fisher's PLSD test after Bartlett test)

Table 4. Mechanical parameters of the fourth lumbar vertebra and the right midfemur in OVX rats treated with risedronate or vitamin K_2

Group	L4		Right femur (midfemur)		
	Ultimate compressive load (N)	Structural modulus (N/mm)	Ultimate bending load (N)	Structural modulus (N/mm)	Material strength (N/mm^2)
1. Sham + vehicle	306.8 ± 40.4	5450 ± 774	173.4 ± 25.0	467.5 ± 58.8	195.6 ± 30.7
2. OVX + vehicle	199.4 ± 54.0*	3631 ± 973*	161.9 ± 17.4	448.5 ± 59.6	184.2 ± 31.0
3. OVX + risedronate 0.1 mg/kg/day	238.5 ± 64.9	4147 ± 1131	170.9 ± 15.6	459.0 ± 52.7	191.3 ± 27.2
4. OVX + risedronate 0.5 mg/kg/day	252.0 ± 34.4**	4551 ± 537**	189.9 ± 21.2***	489.4 ± 53.5	190.3 ± 22.9
5. OVX + risedronate 2.5 mg/kg/day	337.9 ± 69.9***	5760 ± 1026***	193.3 ± 12.9***	512.8 ± 74.4	200.8 ± 11.2
6. OVX + vehicle + vitamin K_2 30 mg/kg/day	226.4 ± 55.7	4038 ± 942	171.4 ± 22.8	479.7 ± 76.0	186.9 ± 16.3
7. OVX + risedronate 0.5 mg/kg/day + vitamin K_2 30 mg/kg/day	275.9 ± 50.1***	4908 ± 709***	203.5 ± 24.7***	477.9 ± 95.9	204.6 ± 21.6

Data are presented as the mean ± SD (n = 9 or 10)
* $P < 0.01$ OVX control (group 2) vs sham control (group 1) (Student's t test); ** $P < 0.05$, *** $P < 0.01$ treated groups (groups 3–7) vs OVX control (group 2) (ANOVA followed by Fisher's PLSD test after Bartlett test)

Table 5. Mineralization properties of the fifth lumbar vertebra and the left midfemur in OVX rats treated with risedronate or vitamin K_2

Group	L5 (trabecular bone)		Left femur (cortical bone)	
	Mineral/matrix ratio	Carbonate/phosphate ratio ($\times 10^3$)	Mineral/matrix ratio	Carbonate/phosphate ratio ($\times 10^3$)
1. Sham + vehicle	7.97 ± 0.71	9.28 ± 0.27	8.88 ± 0.56	10.41 ± 0.69
2. OVX + vehicle	7.01 ± 0.37*	9.00 ± 0.47	9.30 ± 0.65	10.66 ± 0.47
3. OVX + risedronate 0.1 mg/kg/day	7.53 ± 0.59**	9.05 ± 0.42	9.16 ± 0.47	10.67 ± 0.73
4. OVX + risedronate 0.5 mg/kg/day	7.75 ± 0.59***	8.90 ± 0.36	9.05 ± 0.74	10.95 ± 0.48
5. OVX + risedronate 2.5 mg/kg/day	7.72 ± 0.50***	9.16 ± 0.74	9.15 ± 0.65	10.31 ± 1.36
6. OVX + vehicle + vitamin K_2 30 mg/kg/day	7.09 ± 0.65	8.58 ± 0.60	9.13 ± 0.78	10.66 ± 0.74
7. OVX + risedronate 0.5 mg/kg/day + vitamin K_2 30 mg/kg/day	7.82 ± 0.58***	8.72 ± 0.37	9.50 ± 0.83	10.90 ± 0.64

Data are presented as the mean ± SD (n = 9 or 10)
* $P < 0.01$ OVX control (group 2) vs sham control (group 1) (Student's t test); ** $P < 0.05$, *** $P < 0.01$ treated groups (groups 3–7) vs OVX control (group 2) (ANOVA followed by Fisher's PLSD test after Bartlett test)

women with a LS T score of about −1.5 did not seem to further reduce the risk of vertebral fragility fracture in 3 years [40]. If the same is true here, the effect of reduction of turnover by risedronate on bone mechanical properties in OVX rats may be limited at a level not different from that in sham control (normal) rats.

Approximately 12% reduction in mineral-to-matrix ratio in trabecular bone of the rat after OVX is consistent with a previous study [19]. Risedronate prevented, dose-dependently, the OVX-induced decrease in mineral-to-matrix ratio. A dose of tiludronate (35 mg/kg BW) that maintained the lumbar BMD after OVX also prevented the decrease in trabecular mineral-to-matrix ratio [19,41]. Ibandronate, at a dose that did not maintain the trabecular bone mass in ovariohysterectomized beagles, increased the mineral-to-matrix ratio of trabecular bone [18]. Thus, the relationship between the regulation of bone turnover and the mineral-to-matrix ratio of trabecular bone in estrogen deficiency could differ depending on the bisphosphonate and animal model used. It has been observed that mineral-to-matrix ratio is affected in bones of osteonectin-null [42] and osteopontin-null mice [43] and in sodium fluoride-treated minipigs [44,45]. These data indicate that the ratio depends not only on the time period elapsed before the bone tissue can undergo resorption by osteoclasts during remodeling [14,15,18,20], but also on the rate and magnitude of osteoblastic primary bone mineralization. There may be different effects on this osteoclast-to-osteoblast ratio with different bisphosphonates. Carbonate-to-phosphonate ratio did not differ in any groups in our study and others [18,19]. Thus, the parameter may not be a useful measure to assess the effects of OVX or bisphosphonates in rats.

Risedronate increased BMD of the midfemur in OVX rats. This BMD increase was associated with increases in cortical bone area in the cross-sectional morphology of the midfemur. The inhibition of age-dependent increases in midfemur BMD and cross-sectional morphology, including cortical bone area, after OVX has been previously observed [33,35,46,47]. Thus, risedronate administration maintained the age-dependent increases in mass and structure of femoral cortical bone normally lost after OVX. These data are consistent with the effect of other bisphosphonates such as tiludronate and alendronate in OVX rats [33,48]. It is important to note that risedronate did not significantly alter cortical material strength.

Mineral-to-matrix ratio at the center of the femoral cortex did not differ across groups. This result is not surprising, based on previous studies. It has been reported that the turnover at endosteal and periosteal bone surfaces does not affect the central parts of the femoral cortex in SD rats at these ages [33,35]. Similarly, the mineral-to-matrix ratio in the center of the tibia cortex did not significantly differ from 11 weeks up to 9 months of age in mice [42]. These data indicate that the mineral-to-matrix ratio at the central parts of the cortical bone is not influenced by aging and changes in turnover at the bone surfaces in adult rodents, in which intracortical osteonal remodeling is undeveloped. Thus, the mineral-to-matrix ratio in the center of cortical bone in rodents does not depend on the time before undergoing turnover, but is mainly determined during the process of bone formation. Of course, the mineral-to-matrix ratio values at the periosteal or endosteal regions may have reflected the local conditions of bone formation and resorption in the femoral cortex.

In rats treated with vitamin K_2 alone, serum osteocalcin levels were maintained at the levels of sham controls at 9 months after OVX. However, the OVX-induced increase of urinary DPD was not ameliorated by treatment with vitamin K_2. Vitamin K_2 alone did